



Single-cell RNA sequencing reveals the immune microenvironment landscape of osteosarcoma before and after chemotherapy

Yun Liu ^{a,1}, Yunhua Lin ^{b,1}, Shijie Liao ^b, Wenyu Feng ^c, Jianhong Liu ^a, Xiaoting Luo ^d, Qingjun Wei ^{b,**}, Haijun Tang ^{a,*}

^a Department of Spine and Osteopathic Surgery, The First Affiliated Hospital of Guangxi Medical University, Nanning, Guangxi, China

^b Department of Trauma Orthopedic and Hand Surgery, The First Affiliated Hospital of Guangxi Medical University, Nanning, Guangxi, China

^c Department of Orthopedics, The Second Affiliated Hospital of Guangxi Medical University, Nanning, Guangxi, China

^d Department of Pharmacy, The First Affiliated Hospital of Guangxi Medical University, Nanning, Guangxi, China

ARTICLE INFO

Keywords:

Osteosarcoma
Chemotherapy
Tumor immune microenvironment
Single-cell RNA sequencing
Heterogeneity

ABSTRACT

Chemotherapy, a primary treatment for osteosarcoma (OS), has limited knowledge regarding its impact on tumor immune microenvironment (TIME). Here, tissues from 6 chemotherapy-naive OS patients underwent single-cell RNA sequencing (scRNA-seq) and were analyzed alongside public dataset (GSE152048) containing 7 post-chemotherapy OS tissues. CD45⁺ (PTPRC⁺) cells were used for cell clustering and annotation. Changes in immune cell composition pre- and post-chemotherapy were characterized. Totally, 28,636 high-quality CD45⁺ (PTPRC⁺) cells were extracted. Following chemotherapy, the proportions of regulatory T cells (Tregs) and activated CD8 T cells decreased, while CD8 effector T cells increased. GO analysis indicated that differentially expressed genes (DEGs) in T cells were associated with cell activation, adaptive immune response, and immune response to tumor cells. Furthermore, the proportions of plasma cells increased, while naive B cells decreased. B cell surface receptors expression was upregulated, and GO analysis revealed DEGs of B cells were mainly enriched in B cell-mediated immunity and B cell activation. Moreover, M2 polarization of macrophages was suppressed post-chemotherapy. Overall, this study elucidates chemotherapy remodels the OS TIME landscape, triggering immune heterogeneity and enhancing anti-tumor properties.

1. Introduction

Osteosarcoma (OS) is the most common primary malignant tumor of bone, and it occurs mainly in children and adolescents [1,2].

Abbreviations: OS, osteosarcoma; scRNA-seq, single-cell RNA sequencing; TIME, tumor immune microenvironment; follicular helper T, Tfh; CD8 effector T, CD8 Tef; activated CD8 T, Act CD8 T; DEGs, differentially expressed genes; TILs, tumor-infiltrating lymphocytes; PCA, principal component analysis; tSNE, t-distributed random neighbor embeddings; GSEA, gene set enrichment analysis; GO, gene ontology; BP, biological process.

* Corresponding author.

** Corresponding author.

E-mail addresses: weiqingjungxnn@163.com (Q. Wei), haijun2595@163.com (H. Tang).

¹ These authors Contributed equally.

<https://doi.org/10.1016/j.heliyon.2023.e23601>

Received 25 August 2023; Received in revised form 7 December 2023; Accepted 7 December 2023

Available online 11 December 2023

2405-8440/© 2023 The Authors. Published by Elsevier Ltd. This is an open access article under the CC BY-NC-ND license (<http://creativecommons.org/licenses/by-nc-nd/4.0/>).

Despite recent advances in treatment options for OS (surgical resection and chemotherapy), its prognosis remains poor [3]. Hence, there is an urgent need to elucidate the underlying mechanisms involved in OS progression and to identify more effective therapeutic targets to improve the prognosis of OS patients.

The immune components of intra-tumor, also known as the tumor immune microenvironment (TIME), including immune cell types, extracellular immune factors and cell surface molecules, are closely relevant to tumor progression, recurrence and metastasis [4]. Tumor tissues are characterized by extensive heterogeneity, regulated by the metabolic reprogramming of the TIME, which also influences the therapeutic response in different patients [5,6]. Predictably, its characterization is essential to elucidate the therapeutic response of OS patients and guide the treatment strategy option. Chemotherapy has been reported to have a double-edged immunosuppressive and immunostimulatory response to the organism. Favorably for treatment, chemotherapy can remodel TIME and promote immune-mediated tumor killing [7]. Most chemotherapeutic agents have been proven to exert immunostimulatory properties through suppressing immunosuppressive cells or activating effector cells that dysregulate the immunosuppressive microenvironment, thereby increasing immunogenicity and T-cell infiltration [8]. Ryul Kim et al. characterized the effects of standard chemotherapy on gastric cancer (GC) TIME. Their results suggested that chemotherapy-induced M1 macrophage repolarization, NK cell infiltration and effector T cell infiltration were increased among chemotherapy responders [9]. However, the effect of chemotherapy, an important treatment for OS, on OS TIME has not been thoroughly characterized.

Bulk RNA transcriptome sequencing-based studies do not have sufficient resolution in identifying specific cell types and lack resolution of the complex intra-tumor heterogeneity [3]. The availability of single-cell RNA sequencing (scRNA-seq) enables the study of intra-tumor heterogeneity at the single-cell level, thereby revealing the distinct changes for each cell type [4]. Currently, scRNA-seq has been widely used in studies of non-small cell lung cancer (NSCLC), clear cell renal cell carcinoma (ccRCC), and colorectal cancer (CRC), providing a wealth of new insights [10–12]. This study is the first to perform scRNA-seq data analysis on 6 pre-chemotherapy OS tissues and 7 post-chemotherapy OS tissue samples to characterize the impact of chemotherapy on TIME of OS patients and investigate the compositional changes of primary immune cell types and underlying mechanisms pre- and post-chemotherapy. Overall, our present study provides more in-depth insight to explore the TIME characteristics of OS pre- and post-chemotherapy, which can potentially help to develop future treatment strategies to expand the proportion of OS patients benefiting from chemotherapy.

2. Materials and methods

2.1. Acquisition of scRNA-seq data

Samples from 6 patients with osteosarcoma (OS) without chemotherapy were derived from our previous study [13]. All included patients signed the informed consent form, and the study was approved by the Ethics Committee of the First Affiliated Hospital of Guangxi Medical University. Further, we digested the OS tissues and completed sequencing according to our previously reported method [13]. Specifically, the tissue was cut into pieces approximately 1 mm³ size and subsequently rinsed twice using 4 °C Dulbecco's phosphate-buffered saline (DPBS, Thermo Fisher Scientific, Inc.). The tissue was then digested using collagenase 2 (1 mg/mL) at 45 °C and gently shaken for 37 min to prepare the single cell suspension. Further, the single cell suspension was filtered using a 100 mm cell filter, and the filtered suspension was centrifuged at 300 g for 5 min. The suspension was then lysed for 5 min using 1 × erythrocyte lysate (BioLegend, Inc.) and then filtered through a 40 mm cell filter. Immediately afterwards, the single cell suspension was resuspended in DPBS containing 1 % fetal bovine serum (FBS). Cell viability was determined using Trypan Blue staining solution (0.4 %, Thermo Fisher Scientific, Inc.) and cell suspensions with >80 % cell viability were used for the next sequencing procedure. Subsequently, reverse transcription reactions for mRNA and cDNA amplification were performed according to the manufacturer's instructions, and sequencing was further completed on an Illumina HiSeq X Ten instrument (Illumina, Inc.). Upstream single-cell analysis was carried out using cell Ranger (version 4.0.0), and the human genome sequencing reference library GRCh38 was used for the comparison of single-cell sequencing data. The other dataset used in this study, GSE152048, was extracted from the published study conducted by Yan Zhou et al. [3], which contained scRNA-seq data from 7 post-chemotherapy OS tissue samples.

2.2. ScRNA-seq data integration and quality control

ScRNA-seq data was first integrated using the “merge” function provided by the “Seurat” R package (version 4.3.0) [14]. Further, we screened the cells with $nFeature_RNA > 300$, $nFeature_RNA < 4500$, and $percent.mt < 10$ as criteria to exclude low-quality cells. Next, eligible CD45⁺ (PTPRC⁺) cell data were extracted from the processed scRNA-seq data and normalized using the “NormalizeData” function (LogNormalize method) supplied with the “Seurat” R package. Then the “Harmony” R package was utilized to remove the batch effect using the top 30 principal components (PCs) [15].

2.3. Dimensionality reduction and cell clustering of scRNA-seq data

First, the data is scaled using the default parameters of the “ScaleData” function. Then, the “FindVariableFeatures” function in the “Seurat” R package was used to identify the top 2000 variable genes for subsequent analysis. Specifically, $selection.method = “vst”$ and $nfeatures = 2000$ were set as the parameters. To reduce the data dimension, the top 30 principal components were obtained via performing the principal component analysis (PCA) with the default settings of the “RunPCA” function. Next, the “FindNeighbors” and “FindClusters” functions were employed to identify cell clusters, with the resolution set to 0.05, and the results were presented as t-distributed random neighbor embeddings (tSNE).

2.4. Cell annotation, immune cell extraction and subclustering

The identification of differentially expressed genes (DEGs) per cell cluster was conducted using the “FindAllMarkers” function (adjusted $p < 0.05$ and $|\log_2(FC)| > 0.25$ were regarded as criteria). Notely, the parameters of the “FindAllMarkers” function were set as follows: $\text{min.pct} = 0.25$, $\text{logfc.threshold} = 0.25$. Moreover, major immune cell clusters were annotated by comparing the DEGs of each cell cluster with previously reported markers [3,12,16,17], including B cells: CD79A, MZB1; tumor-infiltrating lymphocytes (TILs): NKG7, CD3D; myeloid cells: LYZ and CST3. Thereafter, scRNA-seq data for major immune cell clusters were extracted and further re-clustered into sub-clusters to detect heterogeneity that existed within each cell type. Then, immune cell subclusters were further annotated according to the following cell markers: monocytes: C1QA; macrophages: FCN1; plasma cells: MZB1; naive B cells: IGHD; T cells: CTLA4; NK cells: NKG7, GZMA; Tregs: FOXP3, IL-2RA; follicular helper T cells (Tfh): CXCL13; NKT cells: NCAM1; CD8⁺ effector T cells (CD8⁺ Tef): GZMA; activated CD8⁺ T cells (Act CD8⁺ T): TRAC.

2.5. Chemotherapy-related functional analysis

The “clusterProfiler” R package was utilized to implement the biological process (BP) part of the gene ontology (GO) analysis (using “c5.go.bp.v7.4.symbols.gmt” as the reference gene set) for the identified significant DEGs ($p < 0.05$ and $|\log_2(FC)| > 1$). This allowed us to explore the potential pathways involved in the chemotherapy of primary immune cells. Additionally, gene set enrichment analysis (GSEA) was carried out to assess the relative pathway activity of macrophages pre- and post-chemotherapy. The list of genes characteristic of M2-type macrophages was extracted from the study conducted by Eva M Garrido-Martin et al. [18].

2.6. Statistical analysis

Analysis and visualization of scRNA-seq data were performed using the “Seurat” and “Harmony” R packages. The “clusterProfiler” R package was applied to analyze biological functions pre- and post-chemotherapy. Comparisons of the composition of various immune cell types pre- and post-chemotherapy were performed by chi-square test. Unless otherwise stated, $p < 0.05$ was considered a statistically significant difference.

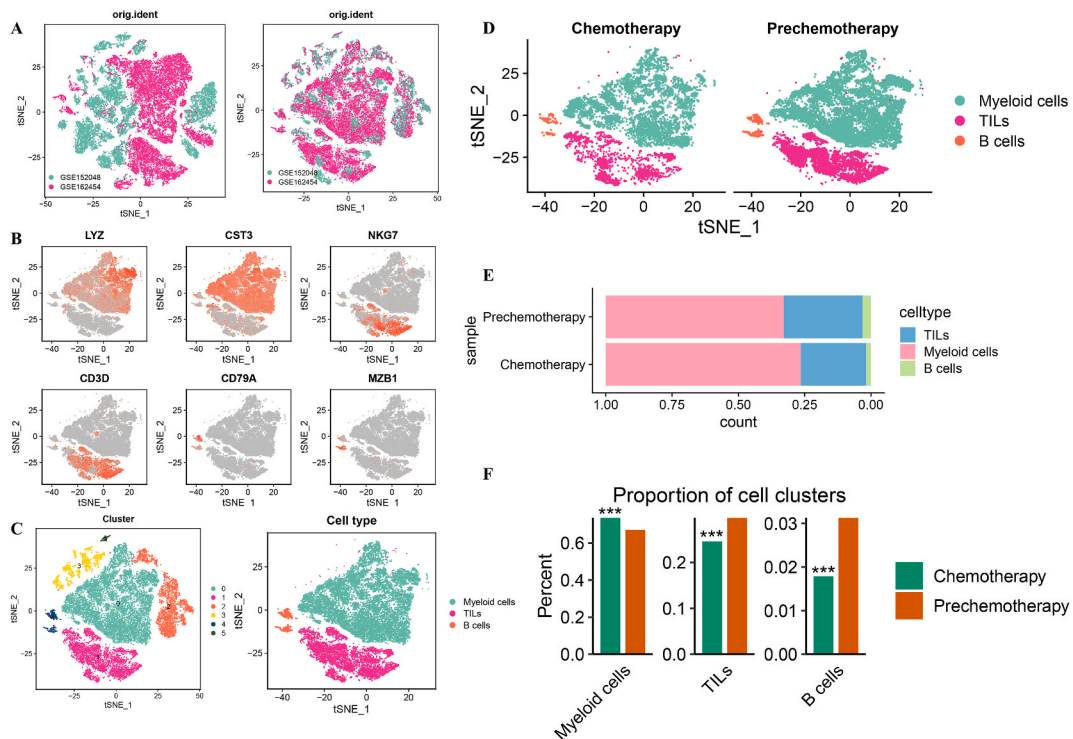


Fig. 1. | Overall single-cell atlas of OS tissues pre- and post-chemotherapy. (A) Elimination of batch effects. The “harmony” R package was implemented to eliminate the batch effect of multiple-source data; (B) Expression of selected marker genes for the definition of 3 primary types of immune cells, namely T cells, B cells and TILs; (C) Cell clustering and annotation as well as extraction of above 3 primary types of immune cells. Different clusters and cell types were presented in different colors; (D) tSNE plot of the above 3 types of immune cells, grouped by pre- and post-chemotherapy; (E) Bar plot, presenting the composition ratio of the above 3 types of immune cells in OS tissue pre- and post-chemotherapy; (F) Difference in the composition ratio of 3 types of immune cells. Compared with OS tissue pre-chemotherapy, *** $p < 0.001$. (For interpretation of the references to color in this figure legend, the reader is referred to the Web version of this article.)

3. Results

3.1. Chemotherapy led to remarkable heterogeneity in OS TIME

After rigorous quality control and elimination of batch effects, a total of 28,636 high-quality CD45⁺ (PTPRC⁺) cells (pre-chemotherapy:18,385 cells, post-chemotherapy:10,251 cells) were derived from 13 samples, which were further dimensionally reduced through implementing the PCA analysis. Cell clustering and annotation were also implemented and then visualized using the t-distributed random neighborhood embedding (tSNE) method (Fig. 1A). This study further investigated 3 major types CD45⁺ (PTPRC⁺) immune cells, including TILs (cluster 1): NKG7, CD3D (n = 7988), B cells (cluster 4): CD79A, MZB1 (n = 758), and myeloid cells (cluster 0): LYZ, CST3 (n = 19890) (Fig. 1B–C). Notably, clusters 2, 3, and 5 were excluded from the follow-up study due to lack of specific expression of these markers. Our findings disclosed that the composition ratio of myeloid cells was significantly increased post-chemotherapy, while the composition ratio of TILs and B cells was significantly decreased post-chemotherapy (Fig. 1D–F, p < 0.001). According to reports, TIL (based on TILs) therapy plays an important role in treating various solid tumors, and the number and activity of TILs are important factors affecting their anti-tumor ability [19,20]. Meanwhile, the role of B cells in anti-tumor immunity is also indispensable [21]. Herein, the decreased composition of the above cells suggests that chemotherapy partly weakens the anti-tumor effects, which may ultimately lead to unsatisfactory treatment outcomes. This reflects that chemotherapy may be detrimental to the immune system to some extent. Still, it is worth noting that chemotherapy has a double-edged sword on the immune system. TILs consist of two components, which play the role of immunoenhancement and immunosuppression factors in anti-tumor immunity, respectively [22]. Thus, it is necessary to conduct an in-depth analysis of the subpopulation composition of primary immune cell types (including TILs, B cell, myeloid cells) and further explore their effects on immunosuppressive factors, which will better elaborate the effects of chemotherapy on the organism [7]. Generally, our findings imply that there was remarkable heterogeneity in OS patients' TIME pre- and post-chemotherapy.

3.2. Chemotherapy reshaped the T-cell population and enhanced anti-tumor properties

To characterize the changes in TILs populations (including NK cells and T cells) pre- and post-chemotherapy, we conducted the subcluster clustering analysis of TILs and acquired 4 cell clusters (Fig. 2A). Among them, clusters 0 and 2 were defined as natural killer

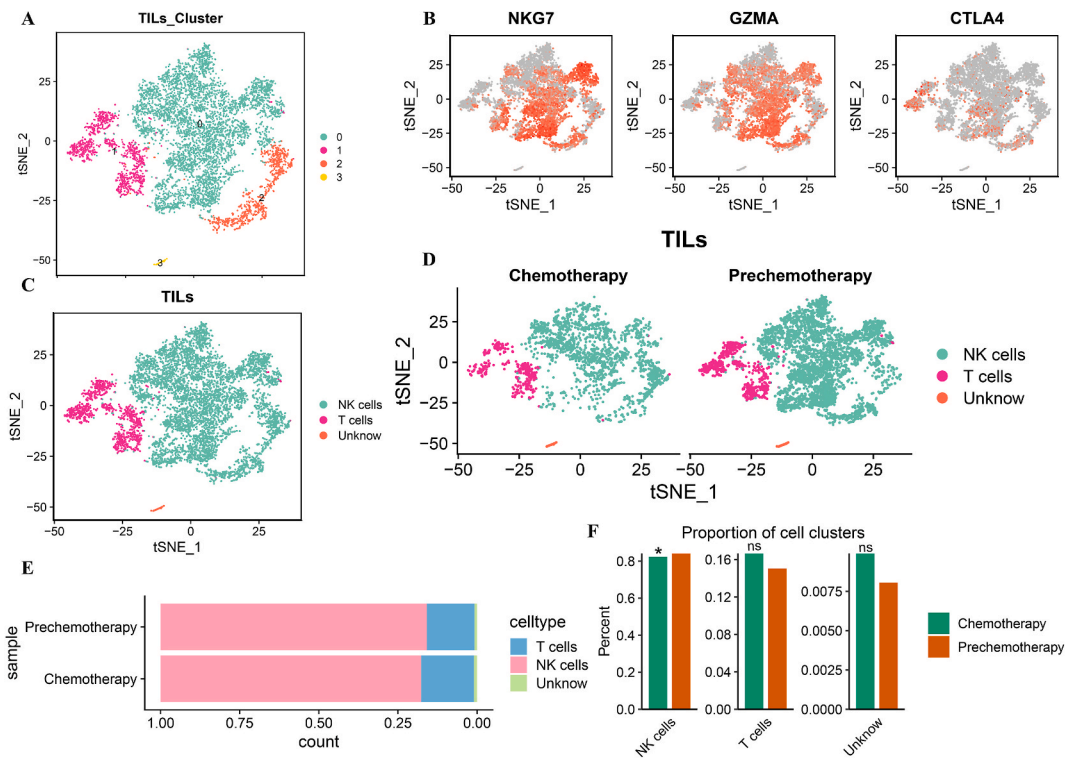


Fig. 2. | Analysis of TILs cluster in OS tissues pre- and post-chemotherapy. (A, C) Re-clustering and subcluster annotation of TILs clusters. Clusters 0 and 2 were defined as NK cells, cluster 1 was defined as T cells, and the cell type of cluster 3 was unknown; (B) Expression of selected marker genes for the definition of the cells, namely T cells, NK cells. (D) tSNE plot of the TILs, grouped by pre- and post-chemotherapy; (E) Bar plot, presenting the composition ratio of the TILs in OS tissue pre- and post-chemotherapy; (F) Difference in the composition ratio of TILs. Compared with OS tissue pre-chemotherapy, *p < 0.05; ns, not significant.

(NK) cells (NKG7, GZMA; n = 6677), accounting for the most TILs. Cluster 1 was defined as T cells (n = CTLA4; n = 1242), and cluster 3 was defined as unknown cell type (n = 69) (Fig. 2B–C). The composition ratio of NK cells significantly decreased post-chemotherapy compared to pre-chemotherapy ($p < 0.05$), while the composition ratio of the other 2 cell populations (including T cells) indicated a consistent tendency to increase post-chemotherapy, despite there was no statistically significant difference ($p > 0.05$) (Fig. 2D–F). To sum up, our present results suggest that the decrease towards the overall composition of the TILs population in OS TIME is primarily attributable to the decrease in NK cells rather than in T cells, which have an integral role in anti-tumor immunity, further revealing the remodeling effect of chemotherapy on the body’s immunity.

Additionally, the re-clustering analysis of T-cell clusters was carried out, thus characterizing their heterogeneity pre- and post-chemotherapy. Here, we identified 2 CD4 T-cell clusters (CD4), 2 CD8 T-cell clusters (CD8A, CD8B) and 1 NKT (NCAM1) cell cluster (Fig. 3A). Regarding CD4 T cell cluster, we defined two sub-cell clusters, including Tregs (FOXP3, IL-2RA) and follicular helper T cells (Tfh) (CXCL13). Regarding CD8 T cell clusters, we also defined two sub-cell clusters, including CD8 effector T cell (CD8 Tef) clusters (CD8A, GZMA) and activated CD8 T cell clusters (Act CD8 T) (TRAC) (Fig. 3B). As presented in Fig. 3C–E, chemotherapy dramatically decreased the composition ratio of CD4 T cells, including Tregs and Tfh ($p < 0.05$ for both). Interestingly, the composition ratio of CD8 Tef cells was significantly increased post-chemotherapy, while Act CD8 T cells presented the opposite trend ($p < 0.001$ for both). Remarkably, the composition ratio of NKT cells presented a trend of increase after chemotherapy, although the difference was not statistically significant. Activated T cells were first reported to undergo epigenetic remodeling, leading to effector functions [23]. Further, under the stimulation of autocrine or paracrine cytokines, activated T cells gradually differentiate into effector T cells or memory T cells. According to our findings, chemotherapy-induced massive transformation of Act CD8 T cells into CD8 Tef cells may be the major contributor of the trend in the composition ratio of the two types of cells, namely Act CD8 T cells and CD8 Tef cells. Similar to our findings, the study conducted by Víctor Sánchez-Margalet et al. also reported that neoadjuvant chemotherapy leads to a reduction of NK cells, CD4 T cells (including Tregs cells) in peripheral blood of breast cancer (BRCA) patients, while CD8 T cells were decreased only in a minority of patients, which was consistent with our results [24]. Other studies also indicate that chemotherapy exerts a similar remodeling effect on T cell populations, thereby enhancing the ability to eliminate tumors [25–27]. Additionally, gene ontology (GO) analysis revealed that DEGs of T cell clusters were primarily enriched in multiple aspects, such as cell activation,

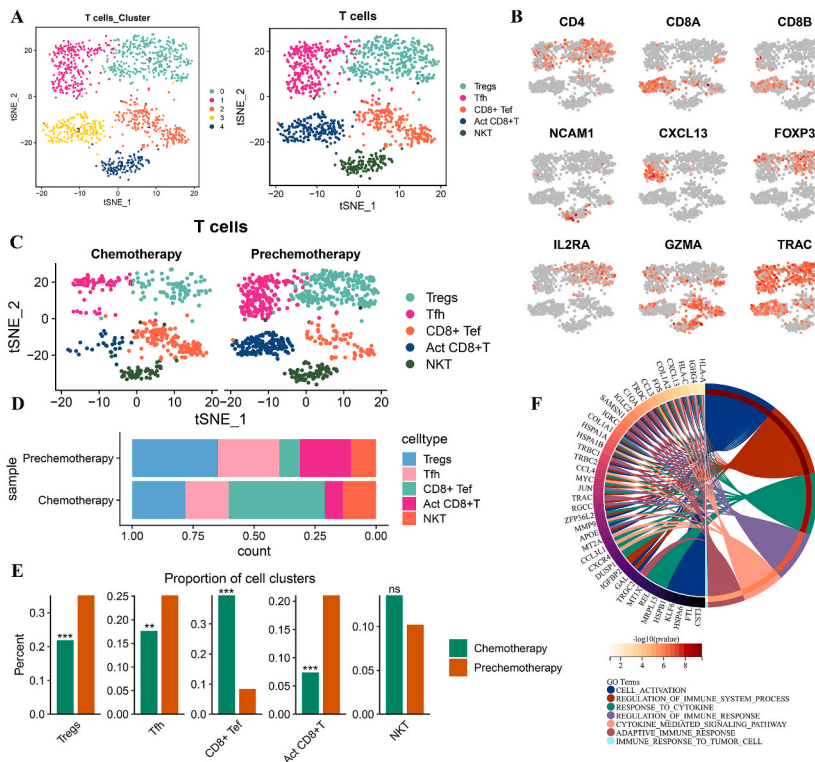


Fig. 3. | Analysis of T cell cluster in OS tissues pre- and post-chemotherapy. (A) Re-clustering and subclusters annotation of T cell cluster. A total of 5 subclusters were defined, namely Tregs, follicular helper T cells (Tfh), CD8 effector T cells (CD8 Tef), and activated CD8 T cells (Act CD8 T); (B) Expression of selected marker genes used to define the cells, with redder color means higher expression (C) tSNE plot of T cell subclusters, grouped by pre- and post-chemotherapy; (D) Bar plot, representing the composition ratios of T cell subclusters in OS tissues pre- and post-chemotherapy; (E) Difference in the composition ratio of T cell subclusters. Compared to OS tissue pre-chemotherapy, ** $p < 0.01$, *** $p < 0.001$; ns, not significant; (F) Underlying pathways involved in T cells pre- and post-chemotherapy revealed through the gene ontology (GO) analysis. “c5.go.bp.v7.4.symbols.gmt” was used as the reference gene set. (For interpretation of the references to color in this figure legend, the reader is referred to the Web version of this article.)

adaptive immune response, and immune response to tumor cells (Fig. 3F). Together, the study’s findings suggest that chemotherapy remodels the T-cell population to provide it improved anti-tumor capabilities. Meanwhile, Yan Zhou et al.’s work has revealed the suppressive status of the immune microenvironment in advanced OS [3]. Combined with our study, it can be seen that chemotherapy partially reverses the immunosuppressive microenvironment. Currently, the application of immunotherapy in OS has received increasing attention, and T cell infiltration plays an essential role in OS immunotherapy [28]. This study suggests that chemotherapy may enhance OS immunotherapy’s efficacy by regulating T cells in the immune microenvironment. Thus, the combination of chemotherapy and immunotherapy may bring promising clinical benefits for OS patients.

3.3. Strong enrichment of plasma cells post-chemotherapy

To further investigate the changes in the composition ratio of B cells, we performed subcluster analysis of B cells and identified 2 subclusters of B cells, including naïve B cells (IGHD; n = 287) and plasma cells (MZB1; n = 471) (Fig. 4A–C). Compared to pre-chemotherapy, the composition ratio of plasma cells increased significantly post-chemotherapy, whereas the percentage composition of naïve B cells decreased (p < 0.05 for both) (Fig. 4D–F). Notably, the current study also revealed that the expression of most BCR genes was significantly increased in B cells after chemotherapy, indicating the enhanced anti-tumor immune response. Moreover, similar results were obtained for the analysis of plasma cells (Fig. 4G). Additionally, GO analysis suggested that DEGs of B cell clusters

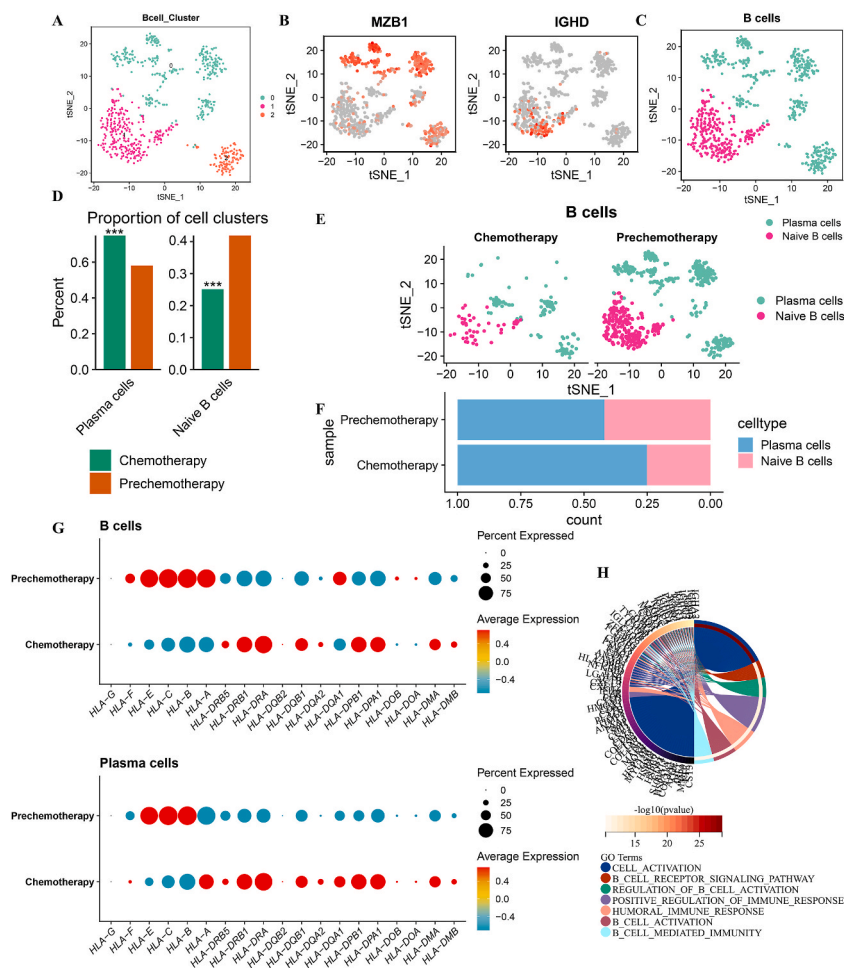


Fig. 4. | Analysis of B cell cluster in OS tissues pre- and post-chemotherapy. (A) Re-clustering of B cell cluster. A total of 3 subclusters were obtained; (B) Expression of selected marker genes used to define the cells, with redder color means higher expression; (C) Subclusters annotation of B cell cluster. Clusters 0 and 2 were defined as plasma cells, and cluster 1 was defined as naïve B cells; (D) Difference in the composition ratio of B cell subclusters; Compared to OS tissue pre-chemotherapy, ***p < 0.001; (E) tSNE plot of B cell subclusters, grouped by pre- and post-chemotherapy; (F) Bar plot, representing the composition ratios of B cell subclusters in OS tissues pre- and post-chemotherapy; (G) Dot plots, demonstrating the expression of B-cell surface receptor (BCR) molecules pre- and post-chemotherapy. Dot size represents the percentage of cells expressing the genes in that group, while redder color means higher expression; (H) Underlying pathways involved in B cells pre- and post-chemotherapy revealed through the gene ontology (GO) analysis. “c5.go.bp.v7.4.symbols.gmt” was used as the reference gene set. (For interpretation of the references to color in this figure legend, the reader is referred to the Web version of this article.)

were mainly enriched in several aspects related to humoral immune activation, such as cell activation, B cell activation, B cell-mediated immunity, and humoral immune response (Fig. 4H). Taken together, post-chemotherapy B cells mainly consisted of plasma cells, suggesting that chemotherapy patients may experience a robust humoral immune response.

3.4. M2 polarization of macrophages was remarkably suppressed post-chemotherapy

We detected a total of 19,890 myeloid cells, representing the vast majority of the total cells. To estimate the heterogeneity of myeloid cells pre- and post-chemotherapy, all myeloid cells were re-clustered into 4 subclusters. Further, cluster 1 was defined as monocytes: C1QA (n = 3889), and cluster 0, 2, and 3 was defined as macrophages: FCN1 (n = 16001) (Fig. 5A–C). Nevertheless, the composition ratios of the two types of cells mentioned above represented no significant difference (p > 0.05, Fig. 5D–F). Interestingly, it has already been reported that neoadjuvant chemotherapy does not alter the monocyte composition of BRCA patients, which was similar to the current findings [24]. Furthermore, the role of macrophages as highly plastic cells with different functions in tumor development has received extensive attention. Briefly, M1 polarization exerts an anti-tumor effect, whereas M2 polarization exerts the opposite pro-tumor effect [29,30]. In our present study, although no remarkable alteration in the composition ratio of macrophages was detected (p > 0.05), the functional status still deserves in-depth investigation. Thus, we further extracted the crucial M2 marker genes and specific M2 gene sets described in previous reports [18]. Notably, the expression levels of M2 marker genes were decreased in OS after chemotherapy (Fig. 5G). As expected, GSEA analysis also disclosed that M2 polarization of macrophages was dramatically inhibited in post-chemotherapy samples (p = 0.02, Fig. 5H). It is worth highlighting that our study achieved consistent results with previous reports [9,18], proving the reliability of our conclusions. Overall, the above findings suggest that chemotherapy may suppress macrophage M2 polarization and thus enhance its anti-tumor effects.

4. Discussion

As a complex system with high heterogeneity, the tumor immune microenvironment (TIME) of osteosarcoma (OS) is closely associated with tumor malignant progression [31]. Previous studies have mainly focused on osteoblasts and osteoclasts, and few

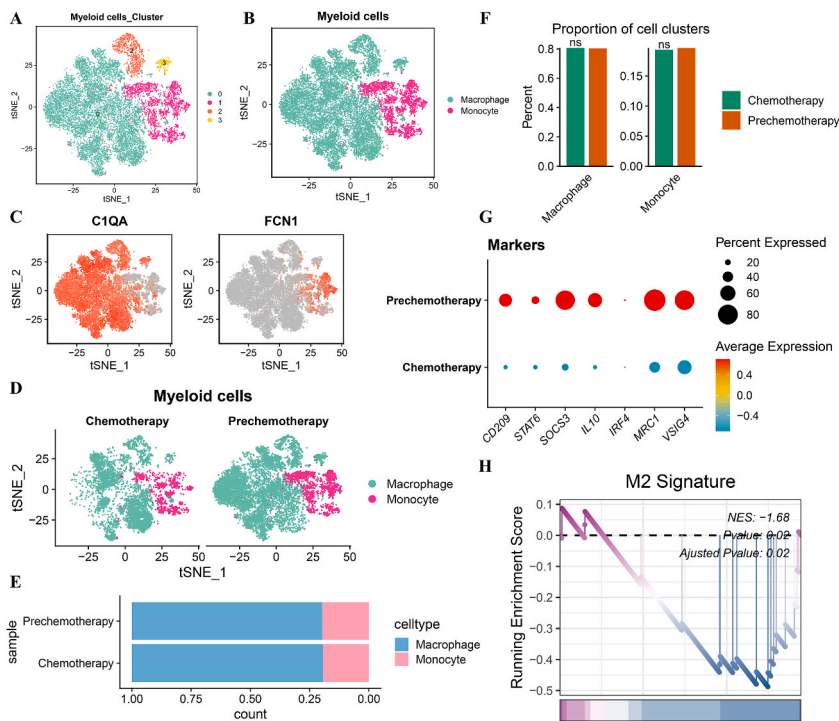


Fig. 5. | Analysis of Myeloid cell cluster in OS tissues pre- and post-chemotherapy. (A) Re-clustering of Myeloid cell cluster. A total of 4 subclusters were obtained; (B) Subclusters annotation of Myeloid cell cluster. Clusters 0, 2, and 3 were defined as macrophages, the cluster 1 was defined as monocytes; (C) Expression of selected marker genes used to define the above cells, with much red representing higher expression; (D) tSNE plot of Myeloid cell subclusters, grouped by pre- and post-chemotherapy; (E) Bar plot, representing the composition ratios of Myeloid cell subclusters in OS tissues pre- and post-chemotherapy; (F) Difference in the composition ratio of Myeloid cell subclusters. Compared to OS tissue pre-chemotherapy, ns represented not significant; (G) Dot plots, demonstrating the expression of M2 macrophage marker genes pre- and post-chemotherapy. Dot size represents the percentage of cells expressing the genes in that group, while redder color means higher expression; (H) Gene enrichment analysis (GSEA) of the specific M2 gene set in macrophages. (For interpretation of the references to color in this figure legend, the reader is referred to the Web version of this article.)

studies have evaluated the whole TIME in OS. Remarkably, studies have reported that the TIME of OS correlates with chemotherapy response [32,33]. However, studies that reported chemotherapy's effect on OS TIME are still lacking. Hence, this study investigated OS TIME before and after chemotherapy using single-cell RNA sequencing (scRNA-seq) analysis. We characterized the landscape of major immune cell types, revealing potential mechanisms of TIME regulation.

T cell-mediated immunity is an essential component of the host's immune response to defend against tumors [34]. Five distinct types of T cells were characterized using the scRNA-seq data analysis, including 2 types of CD4 T cells (Tregs and Tfh), 2 types of CD8 T cells (CD8 Tef and Act CD8 T), and NKT cells. The current findings suggest that the composition ratio of CD4 T cells, including Tregs and Tfh, was dramatically decreased post-chemotherapy, the composition ratio of CD8 Tef cells was dramatically increased post-chemotherapy, while the opposite trend was observed for Act CD8 T cells. Notably, a study has revealed that neoadjuvant chemotherapy mainly resulted in decreased CD4 T cells (including Tregs) in the peripheral blood of BRCA patients, rather than CD8 T cells [24]. This suggests that our current findings are consistent with previous reports. Meanwhile, Treg cells, a type of immunosuppressive cell, were widely reported to exert a suppressive effect in anti-tumor immunity through suppressing the induction and proliferation of effector T cells, thereby inhibiting the function of effector T cells [35–37]. Conversely, activated effector T cells can secrete IL-2, thereby promoting Treg cell expansion [38]. Specifically, Treg cells exert a crucial part in the suppression of T cell-mediated anti-tumor immunity, which is attributed to their suppression of autologous CD4⁺ helper T cells and CD8 Tef [39]. It is well known that CD8 Tef cells are involved in tumor-associated antigen (TAA)-specific immunity, thereby serving an integral part in anti-tumor effect [40]. According to the present findings, we speculated that chemotherapy resulted in a decrease in the composition ratio of Tregs, which would weaken their suppressive effect towards CD8 Tef cells, thus favoring the activation of anti-tumor immunity. As expected, chemotherapy dramatically increased the composition ratio of CD8 Tef cells, suggesting that chemotherapy could activate CD8 Tef cells' capacity to mediate anti-tumor immunity by decreasing the infiltration of suppressive cells—Treg cells in OS TIME. Additionally, GO analysis revealed that the DEGs of T cell cluster were mostly enriched in a variety of aspects, including cell activation and immunological response to tumor cells, which supported the claim that chemotherapy enhanced T cell-mediated anti-tumor immunity.

Furthermore, as observed by Xin Huang et al. [17], myeloid cells (including monocytes, macrophages, etc.) were the most prevalent cell population in OS TIME. Of these, macrophages accounted for a large proportion of myeloid cells. Tumor-associated macrophages (TAM) were commonly considered mainly derived from circulating monocytes [41]. Macrophages were perceived to be immune cells with intrinsic plasticity, and in general, TAM could be classified into M1-like and M2-like phenotypes [4]. M1-like macrophages exert pro-inflammatory and anti-tumor properties, while M2-like macrophages exert the opposite role [18]. M2-like macrophage infiltration was predominant in most solid tumors (including OS) and was associated with poor prognosis [42–48]. Here, no significant heterogeneity in the composition ratio of macrophages was detected pre- and post-chemotherapy, but large differences in their functional status were observed, with chemotherapy modulating the M2 polarization of macrophages. Specifically, the expression levels of M2 marker genes were downregulated in post-chemotherapy OS compared to pre-chemotherapy. The results of the GSEA analysis also indicated that M2 polarization of macrophages was markedly suppressed in post-chemotherapy samples. It has been reported that in mice models of breast cancer and melanoma, paclitaxel reprogrammed the M2 phenotype of TAM to the M1 phenotype with the TLR4-dependent manner, leading to the suppression of tumor growth [49]. In OS, curcumin inhibited M2-polarized macrophages to increase cisplatin (CDDP) sensitivity in OS cells [46]. Combining the current findings with previous reports, we speculate that chemotherapy itself may also inhibit macrophage M2 polarization, thus exerting similar anti-tumor effects, but this needs to be verified by further *in vitro* and *in vivo* experiments.

Additionally, we observed significant heterogeneity in the composition of NK and B cells pre- and post-chemotherapy. Specifically, our findings reveal that chemotherapy decreased the composition ratio of NK and B cells. The above findings were also supported in the study of BRCA chemotherapy [24]. NK cells, a type of intrinsic innate cytolytic effector cell that recognizes and kills tumor cells, have a critical role in innate and adaptive immune responses and tumor immunosurveillance [50,51]. Studies have shown that NK cell infiltration was associated with a good prognosis [52]. Therefore, as the critical component in immunosurveillance, the decreased proportion of NK cells might be a harmful aspect induced by chemotherapy, and hindering this process might be a promising strategy for chemotherapy potentiation; thus, changes in their effector functions warrant further exploration. In this study, the results of subcluster clustering of B-cell populations showed an increase in the percentage of plasma cell composition and a decrease in naive B-cell composition in OS TIME post-chemotherapy. It is generally accepted that plasma cells capable of producing autoantibodies are differentiated from naive B cells [53,54]. Most B cells after chemotherapy are plasma cells, indicating that most naive B cells differentiate into plasma cells. Besides, GO analysis suggested that chemotherapy might be involved in humoral immune activation through multiple pathways, including B-cell activation, B-cell-mediated immunity, and humoral immune response. All of these results suggest that chemotherapy activates a strong humoral immune response.

Currently, it appears that chemotherapy reshapes OS TIME and strengthens the anti-tumor properties of TIME. Although our study provides new insights to explore the effect of chemotherapy on OS TIME, some limitations of the present study must be noted. Firstly, the samples included in this study were limited and unpaired, and the heterogeneity between data from different sources could not be completely eliminated. A larger number of paired samples should be used to validate the results. Secondly, no long-term follow-up data was obtained for the patient. Thirdly, some confounding factors, such as vaccination and infection status, may affect the reliability of conclusions. Additionally, if further *in vivo* and *in vitro* experiments, such as multiplex immunofluorescence and immunohistochemical analysis, are implemented to determine the underlying mechanisms, it will better explain the effect of chemotherapy on OS TIME.

5. Conclusion

In conclusion, this study reveals the dramatic heterogeneity of TIME in OS tissues pre- and post-chemotherapy, characterizes the landscape of primary immune cells, and preliminarily explores the mechanisms. This study provides the first preliminary map of the immune landscape in OS patients post-chemotherapy, which may contribute to the future discovery of precise therapeutic targets to improve OS treatment.

Ethical declaration

The study was approved by the Ethics Committee and Institutional Reviewer Board of the First Affiliated Hospital of the Guangxi Medical University (2019KYK-E-097). The patients/participants were properly informed and provided their written informed consent to participate in this study.

Funding support

This study was supported by Natural Science Foundation of Guangxi Province (2020GXNSFAA259088), Youth Science Foundation of Guangxi Medical University (GXMUYSF202128), Youth Science and Technology Project of the First Affiliated Hospital of Guangxi Medical University (201903038), GuiKe AB22035014/Guangxi Key Research and Development Plan, the National Natural Science Foundation of China (81960768, 82360822, 82260814).

Data availability statement

Data associated with this study has been archived in the Gene Expression Omnibus (GEO) database and is publicly available with the accession number GSE162454 (<https://www.ncbi.nlm.nih.gov/geo/query/acc.cgi?acc=GSE162454>). Additionally, the GSE152048 dataset is also publicly available in the GEO database (<https://www.ncbi.nlm.nih.gov/geo/query/acc.cgi?acc=GSE152048>).

CRedit authorship contribution statement

Yun Liu: Project administration, Funding acquisition, Data curation. **Yunhua Lin:** Writing – original draft, Visualization, Validation, Methodology, Formal analysis, Data curation. **Shijie Liao:** Methodology, Investigation, Data curation, Conceptualization. **Wenyu Feng:** Writing – original draft, Methodology, Formal analysis, Data curation, Conceptualization. **Jianhong Liu:** Writing – original draft, Visualization, Validation, Methodology. **Xiaoting Luo:** Visualization, Methodology, Data curation. **Qingjun Wei:** Writing – review & editing, Validation, Methodology, Funding acquisition. **Haijun Tang:** Writing – review & editing, Visualization, Validation, Investigation, Data curation, Conceptualization.

Declaration of competing interest

The authors declare that they have no known competing financial interests or personal relationships that could have appeared to influence the work reported in this paper.

Acknowledgments

Thanks to all those who supported the implementation of this study.

References

- [1] J. Morrow, I. Bayles, A. Funnell, T. Miller, A. Saiakhova, M. Lizardo, C. Bartels, M. Kapteijn, S. Hung, A. Mendoza, G. Dhillon, D. Chee, J. Myers, F. Allen, M. Gambarotti, A. Righi, A. DiFeo, B. Rubin, A. Huang, P. Meltzer, L. Helman, P. Picci, H. Versteeg, J. Stamatoyannopoulos, C. Khanna, P. Scacheri, Positively selected enhancer elements endow osteosarcoma cells with metastatic competence, *Nat. Med.* 24 (2) (2018) 176–185, <https://doi.org/10.1038/nm.4475>.
- [2] K. Matsuoka, L. Bakiri, L. Wolff, M. Linder, A. Mikels-Vigdal, A. Patiño-García, F. Lecanda, C. Hartmann, M. Sibilia, E. Wagner, Wnt signaling and Loxl2 promote aggressive osteosarcoma, *Cell Res.* 30 (10) (2020) 885–901, <https://doi.org/10.1038/s41422-020-0370-1>.
- [3] Y. Zhou, D. Yang, Q. Yang, X. Lv, W. Huang, Z. Zhou, Y. Wang, Z. Zhang, T. Yuan, X. Ding, L. Tang, J. Zhang, J. Yin, Y. Huang, W. Yu, Y. Wang, C. Zhou, Y. Su, A. He, Y. Sun, Z. Shen, B. Qian, W. Meng, J. Fei, Y. Yao, X. Pan, P. Chen, H. Hu, Single-cell RNA landscape of intratumoral heterogeneity and immunosuppressive microenvironment in advanced osteosarcoma, *Nat. Commun.* 11 (1) (2020) 6322, <https://doi.org/10.1038/s41467-020-20059-6>.
- [4] Y. Bai, D. Chen, C. Cheng, Z. Li, H. Chi, Y. Zhang, X. Zhang, S. Tang, Q. Zhao, B. Ang, Y. Zhang, Immunosuppressive landscape in hepatocellular carcinoma revealed by single-cell sequencing, *Front. Immunol.* 13 (2022), 950536, <https://doi.org/10.3389/fimmu.2022.950536>.
- [5] J. Sung, J. Cheong, New immunometabolic strategy based on cell type-specific metabolic reprogramming in the tumor immune microenvironment, *Cells* 11 (5) (2022), <https://doi.org/10.3390/cells11050768>.
- [6] Y. Yu, P. Fan, J. Li, S. Wang, Preparation of biocompatible manganese selenium-based nanoparticles with antioxidant and catalytic functions, *Molecules* 28 (11) (2023), <https://doi.org/10.3390/molecules28114498>.
- [7] D. Park, M. Robertson-Tessi, K. Luddy, P. Maini, M. Bonsall, R. Gatenby, A. Anderson, The goldilocks window of personalized chemotherapy: getting the immune response just right, *Cancer Res.* 79 (20) (2019) 5302–5315, <https://doi.org/10.1158/0008-5472.Can-18-3712>.
- [8] K. Heinhuis, W. Ros, M. Kok, N. Steeghs, J. Beijnen, J. Schellens, Enhancing antitumor response by combining immune checkpoint inhibitors with chemotherapy in solid tumors, *Ann. Oncol. : official journal of the European Society for Medical Oncology* 30 (2) (2019) 219–235, <https://doi.org/10.1093/annonc/mdy551>.

- [9] R. Kim, M. An, H. Lee, A. Mehta, Y. Heo, K. Kim, S. Lee, J. Moon, S. Kim, B. Min, T. Kim, S. Rha, W. Kang, W. Park, S. Klempner, J. Lee, Early tumor-immune microenvironmental remodeling and response to first-line fluoropyrimidine and platinum chemotherapy in advanced gastric cancer, *Cancer Discov.* 12 (4) (2022) 984–1001, <https://doi.org/10.1158/2159-8290.Cd-21-0888>.
- [10] D. Lambrechts, E. Wauters, B. Boeckx, S. Aibar, D. Nittner, O. Burton, A. Bassez, H. Decaluwé, A. Pircher, K. Van den Eynde, B. Weynand, E. Verbeken, P. De Leyn, A. Liston, J. Vansteenkiste, P. Carmeliet, S. Aerts, B. Thienpont, Phenotype molding of stromal cells in the lung tumor microenvironment, *Nat. Med.* 24 (8) (2018) 1277–1289, <https://doi.org/10.1038/s41591-018-0096-5>.
- [11] C. Krishna, R. DiNatale, F. Kuo, R. Srivastava, L. Vuong, D. Chowell, S. Gupta, C. Vanderbilt, T. Purohit, M. Liu, E. Kansler, B. Nixon, Y. Chen, V. Makarov, K. Blum, K. Attalla, S. Weng, M. Salmans, M. Golkaram, L. Liu, S. Zhang, R. Vijayaraghavan, T. Pawlowski, V. Reuter, M. Carlo, M. Voss, J. Coleman, P. Russo, R. Motzer, M. Li, C. Leslie, T. Chan, A. Hakimi, Single-cell sequencing links multi-regional immune landscapes and tissue-resident T cells in ccRCC to tumor topology and therapy efficacy, *Cancer Cell* 39 (5) (2021) 662–677.e6, <https://doi.org/10.1016/j.ccell.2021.03.007>.
- [12] J. Qi, H. Sun, Y. Zhang, Z. Wang, Z. Xun, Z. Li, X. Ding, R. Bao, L. Hong, W. Jia, F. Fang, H. Liu, L. Chen, J. Zhong, D. Zou, L. Liu, L. Han, F. Ginhoux, Y. Liu, Y. Ye, B. Su, Single-cell and spatial analysis reveal interaction of FAP fibroblasts and SPP1 macrophages in colorectal cancer, *Nat. Commun.* 13 (1) (2022) 1742, <https://doi.org/10.1038/s41467-022-29366-6>.
- [13] Y. Liu, W. Feng, Y. Dai, M. Bao, Z. Yuan, M. He, Z. Qin, S. Liao, J. He, Q. Huang, Z. Yu, Y. Zeng, B. Guo, R. Huang, R. Yang, Y. Jiang, J. Liao, Z. Xiao, X. Zhan, C. Lin, J. Xu, Y. Ye, J. Ma, Q. Wei, Z. Mo, Single-cell transcriptomics reveals the complexity of the tumor microenvironment of treatment-naïve osteosarcoma, *Front. Oncol.* 11 (2021), 709210, <https://doi.org/10.3389/fonc.2021.709210>.
- [14] Y. Hao, S. Hao, E. Andersen-Nissen, W.M. Mauck, S. Zheng, A. Butler, M.J. Lee, A.J. Wilk, C. Darby, M. Zager, P. Hoffman, M. Stoeckius, E. Papalexi, E. P. Mimitou, J. Jain, A. Srivastava, T. Stuart, L.M. Fleming, B. Yeung, A.J. Rogers, J.M. McElrath, C.A. Blish, R. Gottardo, P. Smibert, R. Satija, Integrated analysis of multimodal single-cell data, *Cell* 184 (13) (2021), <https://doi.org/10.1016/j.cell.2021.04.048>.
- [15] I. Korsunsky, N. Millard, J. Fan, K. Slowikowski, F. Zhang, K. Wei, Y. Baglaenko, M. Brenner, P.-R. Loh, S. Raychaudhuri, Fast, sensitive and accurate integration of single-cell data with Harmony, *Nat. Methods* 16 (12) (2019) 1289–1296, <https://doi.org/10.1038/s41592-019-0619-0>.
- [16] L. Peng, X. Jin, B. Li, X. Zeng, B. Liao, T. Jin, J. Chen, X. Gao, W. Wang, Q. He, G. Chen, L. Gong, H. Shen, K. Wang, H. Li, D. Luo, Integrating single-cell RNA sequencing with spatial transcriptomics reveals immune landscape for interstitial cystitis, *Signal Transduct. Targeted Ther.* 7 (1) (2022) 161, <https://doi.org/10.1038/s41392-022-00962-8>.
- [17] X. Huang, L. Wang, H. Guo, W. Zhang, Z. Shao, Single-cell transcriptomics reveals the regulative roles of cancer associated fibroblasts in tumor immune microenvironment of recurrent osteosarcoma, *Theranostics* 12 (13) (2022) 5877–5887, <https://doi.org/10.7150/thno.73714>.
- [18] E. Garrido-Martin, T. Mellows, J. Clarke, A. Ganesan, O. Wood, A. Cazaly, G. Seumois, S. Chee, A. Alzetani, E. King, C. Hedrick, G. Thomas, P. Friedmann, C. Ottensmeier, P. Vijayanand, T. Sanchez-Elsner, M1 tumor-associated macrophages boost tissue-resident memory T cells infiltration and survival in human lung cancer, *Journal for immunotherapy of cancer* 8 (2) (2020), <https://doi.org/10.1136/jitc-2020-000778>.
- [19] M.H. Kazemi, M. Sadri, A. Najafi, A. Rahimi, Z. Baghernejadan, H. Khorramdelazad, R. Falak, Tumor-infiltrating lymphocytes for treatment of solid tumors: it takes two to tango? *Front. Immunol.* 13 (2022), 1018962 <https://doi.org/10.3389/fimmu.2022.1018962>.
- [20] S. Wang, J. Sun, K. Chen, P. Ma, Q. Lei, S. Xing, Z. Cao, S. Sun, Z. Yu, Y. Liu, N. Li, Perspectives of tumor-infiltrating lymphocyte treatment in solid tumors, *BMC Med.* 19 (1) (2021) 140, <https://doi.org/10.1186/s12916-021-02006-4>.
- [21] S. Shalpour, M. Karim, The neglected brothers come of age: B cells and cancer, *Semin. Immunol.* 52 (2021), 101479, <https://doi.org/10.1016/j.smim.2021.101479>.
- [22] S. Arístin Revilla, O. Kranenburg, P.J. Coffey, Colorectal cancer-infiltrating regulatory T cells: functional heterogeneity, metabolic adaptation, and therapeutic targeting, *Front. Immunol.* 13 (2022), 903564, <https://doi.org/10.3389/fimmu.2022.903564>.
- [23] A. Denton, B. Russ, P. Doherty, S. Rao, S. Turner, Differentiation-dependent functional and epigenetic landscapes for cytokine genes in virus-specific CD8+ T cells, *Proc. Natl. Acad. Sci. U.S.A.* 108 (37) (2011) 15306–15311, <https://doi.org/10.1073/pnas.1112520108>.
- [24] V. Sánchez-Margalet, A. Barco-Sánchez, T. Vilarino-García, C. Jiménez-Cortegana, A. Pérez-Pérez, F. Henao-Carrasco, J. Virizuela-Echaburu, E. Nogales-Fernández, M. Álamo-de la Gala, M. Lobo-Acosta, N. Palazón-Carrión, A. Nieto, L. de la Cruz-Merino, Circulating regulatory T cells from breast cancer patients in response to neoadjuvant chemotherapy, *Transl. Cancer Res.* 8 (1) (2019) 59–65, <https://doi.org/10.21037/ter.2018.12.30>.
- [25] M. Peng, Y. Ying, Z. Zhang, L. Liu, W. Wang, Reshaping the pancreatic cancer microenvironment at different stages with chemotherapy, *Cancers* 15 (9) (2023), <https://doi.org/10.3390/cancers15092448>.
- [26] X. Xiang, F. Guo, G. Li, L. Ma, X. Zhu, Z. Abdulla, J. Li, J. Zhang, M. Huang, Efficacy of intra-arterial chemotherapy with sequential anti-PD-1 antibody in unresectable gastric cancer: a retrospective real-world study, *Front. Oncol.* 12 (2022), 1015962, <https://doi.org/10.3389/fonc.2022.1015962>.
- [27] I.J. Rodríguez, D.A. Bernal-Estévez, M. Llano-León, C.E. Bonilla, C.A. Parra-López, Neoadjuvant chemotherapy modulates exhaustion of T cells in breast cancer patients, *PLoS One* 18 (2) (2023), e0280851, <https://doi.org/10.1371/journal.pone.0280851>.
- [28] H. Tian, J. Cao, B. Li, E.C. Nice, H. Mao, Y. Zhang, C. Huang, Managing the immune microenvironment of osteosarcoma: the outlook for osteosarcoma treatment, *Bone Res.* 11 (1) (2023) 11, <https://doi.org/10.1038/s41413-023-00246-z>.
- [29] A. Mantovani, P. Allavena, F. Marchesi, C. Garlanda, Macrophages as tools and targets in cancer therapy, *Nat. Rev. Drug Discov.* 21 (11) (2022) 799–820, <https://doi.org/10.1038/s41573-022-00520-5>.
- [30] M. Pittet, O. Michielin, D. Migliorini, Clinical relevance of tumour-associated macrophages, *Nat. Rev. Clin. Oncol.* 19 (6) (2022) 402–421, <https://doi.org/10.1038/s41571-022-00620-6>.
- [31] T. Zhu, J. Han, L. Yang, Z. Cai, W. Sun, Y. Hua, J. Xu, Immune microenvironment in osteosarcoma: components, therapeutic strategies and clinical applications, *Front. Immunol.* 13 (2022), 907550, <https://doi.org/10.3389/fimmu.2022.907550>.
- [32] S. Martins-Neves, G. Sampaio-Ribeiro, C. Gomes, Chemoresistance-related stem cell signaling in osteosarcoma and its plausible contribution to poor therapeutic response: a discussion that still matters, *Int. J. Mol. Sci.* 23 (19) (2022), <https://doi.org/10.3390/ijms231911416>.
- [33] M. Gerardo-Ramírez, F. Keggenhoff, V. Giam, D. Becker, M. Groth, N. Hartmann, B. Straub, H. Morrison, P. Galle, J. Marquardt, P. Herrlich, M. Hartmann, CD44 contributes to the regulation of MDR1 protein and doxorubicin chemoresistance in osteosarcoma, *Int. J. Mol. Sci.* 23 (15) (2022), <https://doi.org/10.3390/ijms23158616>.
- [34] C. Zhang, L. Lei, X. Yang, K. Ma, H. Zheng, Y. Su, A. Jiao, X. Wang, H. Liu, Y. Zou, L. Shi, X. Zhou, C. Sun, Y. Hou, Z. Xiao, L. Zhang, B. Zhang, Single-cell sequencing reveals antitumor characteristics of intratumoral immune cells in old mice, *Journal for immunotherapy of cancer* 9 (10) (2021), <https://doi.org/10.1136/jitc-2021-002809>.
- [35] Y. Lee, H. Woo, Y. Kim, J. Park, E. Nam, S. Kim, S. Kim, Y. Kim, E. Park, J. Joung, J. Lee, Dynamics of the tumor immune microenvironment during neoadjuvant chemotherapy of high-grade serous ovarian cancer, *Cancers* 14 (9) (2022), <https://doi.org/10.3390/cancers14092308>.
- [36] T. Qi, Y. Luo, W. Cui, Y. Zhou, X. Ma, D. Wang, X. Tian, Q. Wang, Crosstalk between the CBM complex/NF- κ B and MAPK/P27 signaling pathways of regulatory T cells contributes to the tumor microenvironment, *Front. Cell Dev. Biol.* 10 (2022), 911811, <https://doi.org/10.3389/fcell.2022.911811>.
- [37] Y. Xie, F. Xie, L. Zhang, X. Zhou, J. Huang, F. Wang, J. Jin, L. Zhang, L. Zeng, F. Zhou, Targeted anti-tumor immunotherapy using tumor infiltrating cells, *Adv. Sci.* 8 (22) (2021), e2101672, <https://doi.org/10.1002/adv.202101672>.
- [38] G. Ellis, N. Sheppard, J. Riley, Genetic engineering of T cells for immunotherapy, *Nat. Rev. Genet.* 22 (7) (2021) 427–447, <https://doi.org/10.1038/s41576-021-00329-9>.
- [39] N. Zhang, J. Chen, L. Xiao, F. Tang, Z. Zhang, Y. Zhang, Z. Feng, Y. Jiang, C. Shao, Accumulation mechanisms of CD4(+)CD25(+)FOXP3(+) regulatory T cells in EBV-associated gastric carcinoma, *Sci. Rep.* 5 (2015), 18057, <https://doi.org/10.1038/srep18057>.
- [40] Y. Sato, Y. Goto, N. Narita, D. Hoon, Cancer cells expressing toll-like receptors and the tumor microenvironment, *Cancer microenvironment : official journal of the International Cancer Microenvironment Society* (2009) 205–214, <https://doi.org/10.1007/s12307-009-0022-y>.
- [41] D. DeNardo, B. Ruffell, Macrophages as regulators of tumour immunity and immunotherapy, *Nat. Rev. Immunol.* 19 (6) (2019) 369–382, <https://doi.org/10.1038/s41577-019-0127-6>.

- [42] J. Xu, J. Zhang, Z. Zhang, Z. Gao, Y. Qi, W. Qiu, Z. Pan, Q. Guo, B. Li, S. Zhao, X. Guo, M. Qian, Z. Chen, S. Wang, X. Gao, S. Zhang, H. Wang, X. Guo, P. Zhang, R. Zhao, H. Xue, G. Li, Hypoxic glioma-derived exosomes promote M2-like macrophage polarization by enhancing autophagy induction, *Cell Death Dis.* 12 (4) (2021) 373, <https://doi.org/10.1038/s41419-021-03664-1>.
- [43] H. Dan, S. Liu, J. Liu, D. Liu, F. Yin, Z. Wei, J. Wang, Y. Zhou, L. Jiang, N. Ji, X. Zeng, J. Li, Q. Chen, RACK1 promotes cancer progression by increasing the M2/M1 macrophage ratio via the NF- κ B pathway in oral squamous cell carcinoma, *Mol. Oncol.* 14 (4) (2020) 795–807, <https://doi.org/10.1002/1878-0261.12644>.
- [44] Q. Zhang, L. Liu, C. Gong, H. Shi, Y. Zeng, X. Wang, Y. Zhao, Y. Wei, Prognostic significance of tumor-associated macrophages in solid tumor: a meta-analysis of the literature, *PLoS One* 7 (12) (2012), e50946, <https://doi.org/10.1371/journal.pone.0050946>.
- [45] K. Wolf-Dennen, N. Gordon, E. Kleinerman, Exosomal communication by metastatic osteosarcoma cells modulates alveolar macrophages to an M2 tumor-promoting phenotype and inhibits tumoricidal functions, *Oncol Immunology* 9 (1) (2020), 1747677, <https://doi.org/10.1080/2162402x.2020.1747677>.
- [46] J. Wang, J. Jin, T. Chen, Q. Zhou, Curcumol synergizes with cisplatin in osteosarcoma by inhibiting M2-like polarization of tumor-associated macrophages, *Molecules* 27 (14) (2022), <https://doi.org/10.3390/molecules27144345>.
- [47] J. Liang, J. Chen, S. Hua, Z. Qin, J. Lu, C. Lan, Bioinformatics analysis of the key genes in osteosarcoma metastasis and immune invasion, *Transl. Pediatr.* 11 (10) (2022) 1656–1670, <https://doi.org/10.21037/tp-22-402>.
- [48] Z. Luo, P. Liu, Z. Wang, C. Chen, H. Xie, Macrophages in osteosarcoma immune microenvironment: implications for immunotherapy, *Front. Oncol.* 10 (2020), 586580, <https://doi.org/10.3389/fonc.2020.586580>.
- [49] C. Wanderley, D. Colón, J. Luiz, F. Oliveira, P. Viacava, C. Leite, J. Pereira, C. Silva, C. Silva, R. Silva, C. Speck-Hernandez, J. Mota, J. Alves-Filho, R. Lima-Junior, T. Cunha, F. Cunha, Paclitaxel reduces tumor growth by reprogramming tumor-associated macrophages to an M1 profile in a TLR4-dependent manner, *Cancer Res.* 78 (20) (2018) 5891–5900, <https://doi.org/10.1158/0008-5472.Can-17-3480>.
- [50] Y. Sun, L. Li, W. Yao, X. Liu, Y. Yang, B. Ma, D. Xue, USH2A mutation is associated with tumor mutation burden and antitumor immunity in patients with colon adenocarcinoma, *Front. Genet.* 12 (2021), 762160, <https://doi.org/10.3389/fgene.2021.762160>.
- [51] W. Dong, X. Wu, S. Ma, Y. Wang, A. Nalin, Z. Zhu, J. Zhang, D. Benson, K. He, M. Caligiuri, J. Yu, The mechanism of anti-PD-L1 antibody efficacy against PD-L1-negative tumors identifies NK cells expressing PD-L1 as a cytolytic effector, *Cancer Discov.* 9 (10) (2019) 1422–1437, <https://doi.org/10.1158/2159-8290.Cd-18-1259>.
- [52] J. Jones, W. Moody, J. Shields, Microenvironmental modulation of the developing tumour: an immune-stromal dialogue, *Mol. Oncol.* 15 (10) (2021) 2600–2633, <https://doi.org/10.1002/1878-0261.12773>.
- [53] S. Ramon, S. Bancos, C. Serhan, R. Phipps, Lipoxin A₄ modulates adaptive immunity by decreasing memory B-cell responses via an ALX/FPR2-dependent mechanism, *Eur. J. Immunol.* 44 (2) (2014) 357–369, <https://doi.org/10.1002/eji.201343316>.
- [54] Z. Dong, Z. Liu, H. Dai, W. Liu, Z. Feng, Q. Zhao, Y. Gao, F. Liu, N. Zhang, X. Dong, X. Zhou, J. Du, G. Huang, X. Tian, B. Liu, The potential role of regulatory B cells in idiopathic membranous nephropathy, *Journal of immunology research* 2020 (2020), 7638365, <https://doi.org/10.1155/2020/7638365>.